Preprint of: Journal of Biomechanics, Volume 47, Issue 6, 11 April 2014,

Pages 1531–1536, doi:10.1016/j.jbiomech.2014.02.009

Hill-type muscle model with serial damping and eccentric force-velocity relation

D.F.B. Haeufle

Universität Stuttgart, Institut für Sport- und Bewegungswissenschaft, Allmandring 28, D-70569 Stuttgart, Germany.

M. Günther

Universität Stuttgart, Institut für Sport- und Bewegungswissenschaft, Allmandring 28, D-70569 Stuttgart, Germany.

Friedrich Schiller Universität, Institut für Sportwissenschaft, Seidelstrasse 20, D-07743 Jena, Germany.

A. Bayer

Universität Stuttgart, Institut für Sport- und Bewegungswissenschaft, Allmandring 28, D-70569 Stuttgart, Germany.

S. Schmitt

Universität Stuttgart, Institut für Sport- und Bewegungswissenschaft, Allmandring 28, D-70569 Stuttgart, Germany.

Universität Stuttgart, Stuttgart Research Centre for Simulation Technology (SRC SimTech), Pfaffenwaldring 5a, D-70569 Stuttgart, Germany.

Abstract

Hill-type muscle models are commonly used in biomechanical simulations to predict passive and active muscle forces. Here, a model is presented which consists of four elements: a contractile element with force-length and force-velocity relations for concentric and eccentric contractions, a parallel elastic element, a series elastic element, and a serial damping element. With this, it combines previously published effects relevant for muscular contraction, i.e. serial damping and eccentric force-velocity relation. The model is exemplarily applied to arm movements. The more realistic representation of the eccentric force-velocity relation results in human-like elbow-joint flexion. The model is provided as ready to use Matlab® and Simulink® code.

Keywords: muscle; model; serial damping; eccentric contraction; force-velocity relation; multi-body simulation

1. Introduction

Hill-type muscle models are commonly used in biomechanical simulations to predict passive and active muscle forces during various movements. They predict muscle forces on an organ level and are therefore considered macroscopic muscle models. In mechanics, Hill-type muscle models are classified as 0-d elements due to the lack of mass and inertia. Such a model's output is a one-dimensional force, which is applied to skeletal models between origin and insertion points, or sometimes as moments by means of (constant) lever arms. The models' inputs are muscle length, or more precisely muscle-tendon-complex (MTC) length, MTC contraction velocity, and neural muscle stimulation. Typically, Hill-type muscle models consist of three elements: a contractile element incorporating force-length and force-velocity dependencies, a serial and a parallel elastic element in diverse configurations [30, 29, 27, 5, 10, 14, 25]. Various extensions account for physiologically observable effects, such as contraction history effects [17, 21, 16], recruitment patterns of slow- and fast twitch fibers [28], high frequency oscillation damping [6, 24], or force in eccentric contractions [27, 4, 26]. The model presented here combines the latter two.

In eccentric contractions the muscle is elongated due to external forces exceeding the force the muscle is currently generating. In contrast to the extensively studied concentric contractions, considerably less data has been published on eccentric contractions – presumably due to the experimental difficulties. It has, however, been observed that during eccentric contractions single muscle fibers and whole muscles produce forces exceeding

Email address: daniel.haeufle@inspo.uni-stuttgart.de (D.F.B. Haeufle)

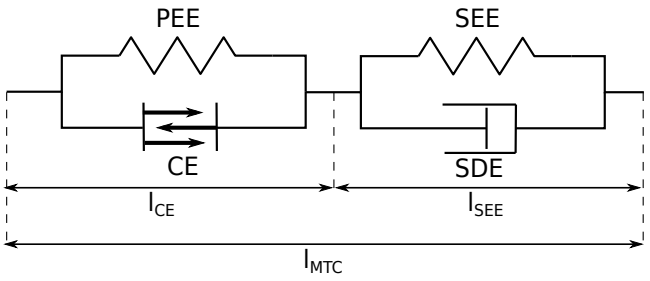

Figure 1: The structure of the MTC model. l_{MTC} is the sum of the length of the contractile element (CE) l_{CE} plus the length of the serial elastic element (SEE) l_{SEE}. The length of the parallel elastic element (PEE) equals l_{CE}. The serial damping component SDE was introduced by Günther et al. [6].

those of isometric (at constant length) contractions [12, 11, 20, 26]. Furthermore, the eccentric muscle force depends on the contraction velocity. For small lengthening velocities, the force rapidly increases with increasing velocities [12, 11, 20, 26]. For higher lengthening velocities (where the experimental difficulties increase, e.g., due to fiber damage) some studies report force saturation [11], a slower increase in force [26], or even a slow reduction with increasing lengthening velocity, depending on the experimental setup. Van Soest and Bobbert [1993] proposed a muscle model where the eccentric force-velocity relation is described by a hyperbolic relation. The advantages of this approach are the possibility to use similar equations for concentric and eccentric force-velocity relation and the good approximation of the experimental data.

The biomechanical function of the eccentric force-velocity relation has also been examined. Seyfarth et al. [23] showed in a simulation study that the jumping performance of long jumps is greatly influenced by the eccentric force-velocity relation. Here, a key feature is the relatively low metabolic energy required for relatively high eccentric forces [15]. Also, the increased muscle force in eccentric contractions together with the reduced force in concentric contractions can have an effect similar to a mechanical damper. With this, the muscle can dissipate movement energy, e.g. during down-hill walking [15], and provide rapid stabilizing reactions to perturbations in hopping [8].

Günther et al. [6] found, that the low but significant damping within the passive tendinous tissue [13, 1] is responsible for the dampening of high-frequency oscillations. Considering such a damping in the series elastic structure of a Hill-type muscle model predicts muscle forces more realistically. Otherwise, unrealistic high frequency oscillations may occur when simulating contractions against a mass [6].

For complex biomechanical simulations of human movement, both series elastic damping and the characteristic eccentric force-velocity relation have to be considered. Here, we propose a Hill-type model based on van Soest and Bobbert [27], Günther et al. [6], and Mörl et al. [18], which models both effects. Furthermore, we propose a robust method to find the initial conditions for the muscle model's internal state. With these extensions, the muscle model can be used in multi-body simulations of many different human and animal movements. We provide the model implemented in Matlab®/Simulink® as electronic supplementary material and hope, that this facilitates the biomechanical research on biological movement.

2. Muscle model

The model of the muscle tendon complex (MTC) consists of four elements (see Fig. 1): the contractile element (CE) modeling the active force production, the parallel elastic element (PEE) arranged in parallel to the CE, the serial elastic element (SEE) in series to the CE (length l_{SEE}), and the serial damping element (SDE) in parallel to the SEE. The four elements fulfill the force equilibrium

$$F_{CE}(l_{CE}, \dot{l}_{CE}, q) + F_{PEE}(l_{CE}) = F_{SEE}(l_{CE}, l_{MTC}) + F_{SDE}(l_{CE}, \dot{l}_{CE}, \dot{l}_{MTC}, q) \ . \tag{1}$$

In this equation, the force dependencies are also specified. l and $\dot{l}$ with the respective subscripts symbolize length and contraction velocity of the respective elements. $q_0 \leq q \leq 1$ represents the muscles activity with $q = q_0 = 0.001$ for minimally activated muscle and $q = 1$ for maximally activated muscle. The lower limit $q_0 > 0$ captures the fact that in a whole muscle with it's vast number of contractile proteins some cross bridges will always generate force even in the absence of neural stimulation. Additionally, the model's equations generate a singularity for $q = 0$ – the lower limit is thus a precondition for the simulation. The elements' forces in Eq. (1) will be explicitly formulated in the following paragraphs. The kinematic relations between the elements are $l_{SEE} = l_{SDE}$, $l_{PEE} = l_{CE}$, and $l_{MTC} = l_{SEE} + l_{CE}$.

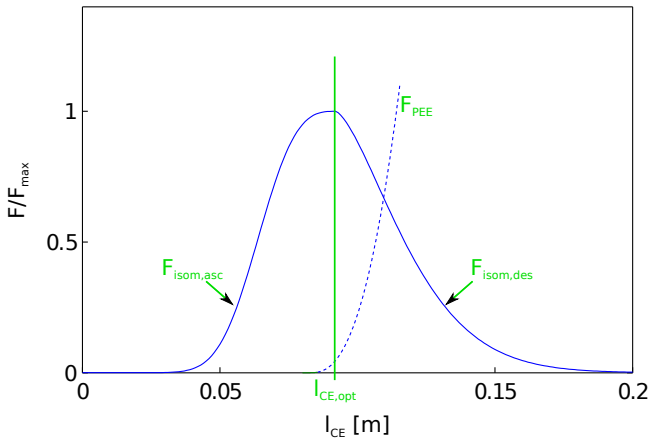

Figure 2: Force-length relation of the contractile element (CE, solid line) and the parallel elastic element (PEE, dashed line) starting at $0.95 \cdot l_{CE,opt}$.

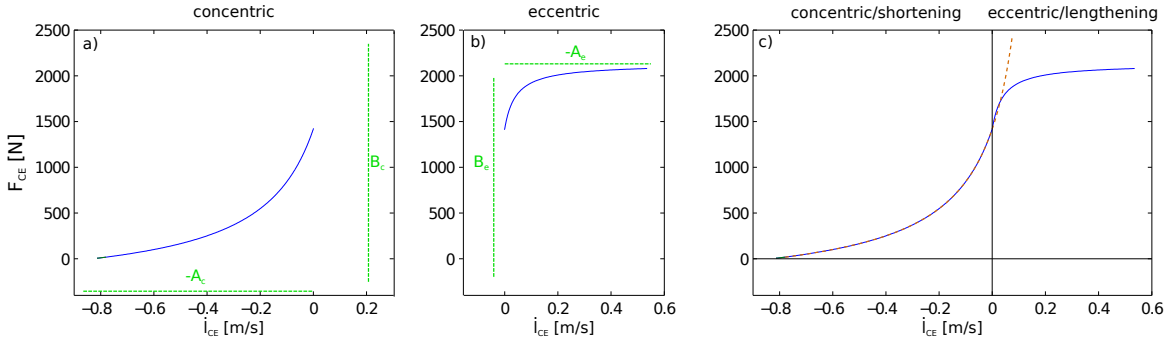

Figure 3: Force-velocity relation of the contractile element (CE). a) For concentric contractions [6] and b) the new extension for eccentric contractions based on van Soest and Bobbert [27]. c) comparison of the new force-velocity relation (solid line) to the previous (dashed line, [6]). Also shown are the hyperbolas' asymptotes $-A = -A_{rel} F_{max}$ and $B = B_{rel} l_{CE,opt}$.

2.1. Contractile element CE

The contractile element CE represents the active fiber bundles in the muscle. The CE force depends on the current length of the muscle fibers. This *force-length relation* (Fig. 2) is modeled as

$$F_{isom}(l_{CE}) = \exp\left\{ -\left| \frac{l_{CE}/l_{CE,opt} - 1}{\Delta W_{limb}} \right|^{\nu_{CE,limb}} \right\} \tag{2}$$

Here, $l_{CE,opt}$ is the optimal fibre length for which $F_{isom}(l_{CE,opt})$ reaches a maximum. ΔW_{limb} depicts the width of the normalized bell curve in the respective limb (ascending or descending) and $\nu_{CE,limb}$ its exponent.

Furthermore, the CE force depends on the current fiber contraction velocity $\dot{l}_{CE}$ (with $\dot{l}_{CE} < 0$ for concentric contractions, indicated by the index "c"). This *force-velocity relation* [9] is modeled as a hyperbola (see Fig. 3a)

$$F_{CE,c}(\dot{l}_{CE} \leq 0) = F_{max} \left(\frac{q F_{isom} + A_{rel}}{1 - \frac{\dot{l}_{CE}}{B_{rel} l_{CE,opt}}} - A_{rel} \right) \quad . \tag{3}$$

The parameters A_{rel} and B_{rel} are the normalized Hill "parameters" [9]. $F_{\max}$ is the maximum isometric force.

As shown by experiments and previously described [29, 27, 6], the Hill parameters depend on length l_{CE} and activation q: $A_{rel}(l_{CE}, q) = A_{rel,0}\, L_{A_{rel}}(l_{CE})\, Q_{A_{rel}}(q)$ and $B_{rel}(l_{CE}, q) = B_{rel,0}\, L_{B_{rel}}(l_{CE})\, Q_{B_{rel}}(q)$. The dependencies are modeled as

$$L_{A_{rel}}(l_{CE}) = \begin{cases} 1 & , l_{CE} < l_{CE,opt} \\ F_{isom}(l_{CE}) & , l_{CE} \geq l_{CE,opt} \end{cases} \tag{4}$$

$$L_{B_{rel}}(l_{CE}) = 1. \tag{5}$$

and

$$Q_{A_{rel}}(q) = \frac{1}{4}(1 + 3\,q) \tag{6}$$

$$Q_{B_{rel}}(q) = \frac{1}{7}(3 + 4\,q). \tag{7}$$

In the previously published versions of this model [6, 18], the force-velocity relation as described above was not explicitly modeled for eccentric contractions ($\dot{l}_{CE} > 0$, lengthening muscle, indicated by the index "e"). The relation given in Eq. (3) would also give a result for $\dot{l}_{CE} > 0$ (see Fig. 3c, dashed line), which, however, deviates from experimental findings. Here, the model was extended for eccentric contractions (see Fig. 3b).

The eccentric force-velocity relation can also be described by a hyperbola [27]. For this approach, Eq. (3) was used, only with $A_{rel,e}$ and $B_{rel,e}$ as the hyperbola parameters for the eccentric branch

$$F_{CE,e}(\dot{l}_{CE} > 0) = F_{max}\left(\frac{qF_{isom} + A_{rel,e}}{1 - \frac{\dot{l}_{CE}}{B_{rel,e} l_{CE,opt}}} - A_{rel,e}\right) \quad . \tag{8}$$

The eccentric hyperbola has to continuously extend the concentric branch at $\dot{l}_{CE} = 0$, which is already fulfilled by Eq. (8) as the term qF_{isom} is the same as in the concentric branch. To define $A_{rel,e}$ and $B_{rel,e}$, two additional constraints are required [27]. The ratio of the derivatives of the force-velocity relation at the transition point (isometric condition $\dot{l}_{CE} = 0$) can be described by one parameter S_e

$$\left.\frac{dF_{CE,e}}{d\dot{l}_{CE}}\right|_{\dot{l}_{CE}=0} = S_e \left.\frac{dF_{CE,c}}{d\dot{l}_{CE}}\right|_{\dot{l}_{CE}=0} \quad . \tag{9}$$

Also, the asymptotic force approached for high eccentric velocities can be defined as $F_{CE} \to F_e qF_{isom}F_{\max}$ for $\dot{l}_{CE} \to +\infty$. Thus, we find

$$A_{rel,e} = -F_e qF_{isom} \quad . \tag{10}$$

$B_{rel,e}$ can now be derived from Eq. (9). Inserting the derivatives, Eq. (9) writes

$$F_{max}\left.\frac{-(qF_{isom} + A_{rel,e})\frac{1}{B_{rel,e} l_{CE,opt}}}{(1 - \frac{\dot{l}_{CE}}{B_{rel,e} l_{CE,opt}})^2}\right|_{\dot{l}_{CE}=0} = S_e\, F_{max}\left.\frac{-(qF_{isom} + A_{rel})\frac{1}{B_{rel} l_{CE,opt}}}{(1 - \frac{\dot{l}_{CE}}{B_{rel} l_{CE,opt}})^2}\right|_{\dot{l}_{CE}=0} \quad .$$

Evaluating the equation in the isometric condition $\dot{l}_{CE} = 0$, i.e. at $F_{CE} = F_{CE,e} = qF_{isom}F_{\max}$, solving for $B_{rel,e}$ and inserting Eq. (10), results in

$$\begin{aligned} \frac{qF_{isom} + A_{rel,e}}{B_{rel,e}} &= S_e \frac{qF_{isom} + A_{rel}}{B_{rel}} \\ \Leftrightarrow B_{rel,e} &= \frac{B_{rel}\,(qF_{isom} + A_{rel,e})}{S_e\,(qF_{isom} + A_{rel})} \\ &= \frac{B_{rel}\,(1 - F_e)}{S_e\left(1 + \frac{A_{rel}}{qF_{isom}}\right)} \quad . \end{aligned} \tag{11}$$

The resulting eccentric force-velocity relation is shown in Fig. 3b. The difference to the previous models is depicted in Fig. 3c.

2.2. Parallel elastic element PEE

The characteristics of the parallel elastic element are modeled as

$$F_{PEE}(l_{CE}) = \begin{cases} 0 & , l_{CE} < l_{PEE,0} \\ K_{PEE}\,(l_{CE} - l_{PEE,0})^{\nu_{PEE}} & , l_{CE} \geq l_{PEE,0} \end{cases} \tag{12}$$

with $K_{PEE} = \mathcal{F}_{PEE}\,\frac{F_{max}}{(l_{CE,opt}\,(\Delta W_{limb=des} + 1 - \mathcal{L}_{PEE,0}))^{\nu_{PEE}}}$ and $l_{PEE,0} = \mathcal{L}_{PEE,0}\,l_{CE,opt}$ with the three free parameters $\mathcal{F}_{PEE}$, $\mathcal{L}_{PEE,0}$ and ν_{PEE} [6].

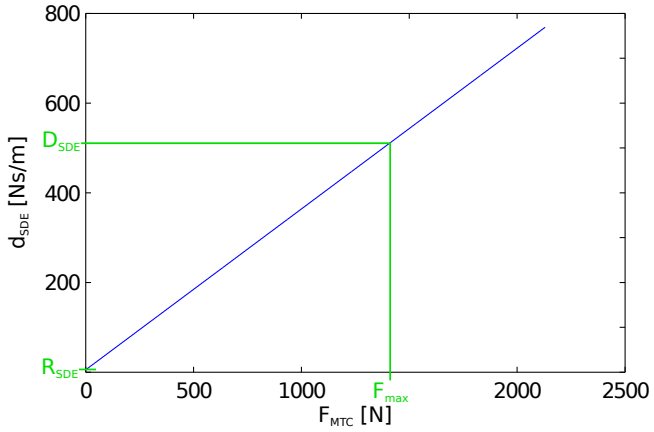

Figure 4: The damping coefficient d_{SDE} linearly depends on the the muscle tendon force F_{MTC}. R_{SDE} is the minimal damping coefficient for $F_{MTC} = 0$. $D_{SDE,max}$ is the damping coefficient at $F_{MTC} = F_{\max}$.

2.3. Serial damping element SDE

The serial damping element force

$$\begin{aligned} &F_{SDE}(l_{CE}, \dot{l}_{CE}, \dot{l}_{MTC}, q) = \\ &D_{SDE,max} \cdot \left((1 - R_{SDE}) \cdot \frac{F_{CE}(l_{CE}, \dot{l}_{CE}, q) + F_{PEE}(l_{CE})}{F_{max}} + R_{SDE}\right) \cdot \left(\dot{l}_{MTC} - \dot{l}_{CE}\right) \end{aligned} \tag{13}$$

is a viscous damper-like force, with a damping coefficient depending on the muscle output force $F_{MTC} = F_{CE}(l_{CE}, \dot{l}_{CE}, q) + F_{PEE}(l_{CE})$ [18]. The parameter $R_{SDE} \leq 1$ represents the damping at $F_{MTC} = 0$, the multiplier $D_{SDE,max}$ the maximum damping coefficient at $F_{MTC} = F_{\max}$ (see Fig. 4).

2.4. Serial elastic element SEE

The force F_{SEE} acting in the serial elastic element (SEE) is modeled by a non-linear toe zone with a linear continuation [6]:

$$F_{SEE}(l_{SE}) = \begin{cases} 0 & , l_{SE} < l_{SEE,0} \\ K_{SEE,nl}\,(l_{SE} - l_{SEE,0})^{\nu_{SEE}} & , l_{SE} < l_{SEE,nll} \\ \Delta F_{SEE,0} + K_{SEE,l}\,(l_{SE} - l_{SEE,nll}) & , l_{SE} \geq l_{SEE,nll} \end{cases} \tag{14}$$

All parameters introduced in Eq. (14) can be derived from the parameters $l_{SEE,0}$ (rest length), $\Delta U_{SEE,nll}$ (relative stretch at non-linear–linear transition), $\Delta F_{SEE,0}$ (both force at the transition and force increase in the linear part), and $\Delta U_{SEE,l}$ (relative additional stretch in the linear part providing a force increase of $\Delta F_{SEE,0}$):

$$\begin{aligned} l_{SEE,nll} &= (1 + \Delta U_{SEE,nll})\, l_{SEE,0} \\ \nu_{SEE} &= \Delta U_{SEE,nll} / \Delta U_{SEE,l} \\ K_{SEE,nl} &= \Delta F_{SEE,0} / (\Delta U_{SEE,nll}\, l_{SEE,0})^{\nu_{SEE}} \\ K_{SEE,l} &= \Delta F_{SEE,0} / (\Delta U_{SEE,l}\, l_{SEE,0}) \quad . \end{aligned}$$

2.5. Contraction dynamics

In a multi-body simulation, the input to the muscle model is the muscle length l_{MTC}, the contraction velocity $\dot{l}_{MTC}$. We can also assign a value to the activity q as the second CE state variable. The time development of the internal degree of freedom (l_{CE}) can now be calculated by solving the differential equation

$$\dot{l}_{CE} = \dot{l}_{CE}(l_{CE}, l_{MTC}, \dot{l}_{MTC}, q) \ . \tag{15}$$

This differential equation can be formulated by solving the force equilibrium (Eq. (1)) for $\dot{l}_{CE}$, ending up with a quadratic equation in $\dot{l}_{CE}$ [6, 18]:

$$0 = C_2 \cdot \dot{l}_{CE}^2 + C_1 \cdot \dot{l}_{CE} + C_0 \tag{16}$$

The coefficients are

$$\begin{aligned} C_2 &= d_{SE,max}(l_{CE}, q) \cdot \left(R_{SE} - \left(A_{rel}(l_{CE}, q) - \frac{F_{PEE}(l_{CE})}{F_{max}}\right) \cdot (1 - R_{SE})\right) \\ C_1 &= -\left(C_2 \cdot \dot{l}_{MTC} + D_0 + F_{SEE}(l_{MTC}, l_{CE}) - F_{PEE}(l_{CE}) + F_{max} \cdot A_{rel}(l_{CE}, q)\right) \\ C_0 &= D_0 \cdot \dot{l}_{MTC} + l_{CE,opt} \cdot B_{rel}(l_{CE}, q) \cdot (F_{SEE}(l_{MTC}, l_{CE}) - F_{PEE}(l_{CE}) - F_{max} \cdot q \cdot F_{isom}(l_{CE})) \end{aligned} \tag{17}$$

using

$$D_0 = l_{CE,opt} \cdot B_{rel}(l_{CE}, q) \cdot d_{SE,max}(l_{CE}, q) \cdot \left(R_{SE} + (1 - R_{SE}) \cdot \left(q \cdot F_{isom}(l_{CE}) + \frac{F_{PEE}(l_{CE})}{F_{max}} \right) \right) \quad (18)$$

as an abbreviation. The appropriate solution of Eq. (16)

$$\dot{l}_{CE} = \begin{cases} \frac{-C_1 - \sqrt{C_1^2 - 4 \cdot C_2 \cdot C_0}}{2 \cdot C_2} & \dot{l}_{CE} \leq 0 \\ \frac{-C_{1,e} + \sqrt{C_{1,e}^2 - 4 \cdot C_{2,e} \cdot C_{0,e}}}{2 \cdot C_{2,e}} & \dot{l}_{CE} > 0 \end{cases} \quad (19)$$

depends on whether the muscle operates in concentric or eccentric mode. $C_{1,e}$, $C_{2,e}$, and $C_{3,e}$ indicate, that all instances of A_{rel} and B_{rel} in the coefficients (Eq. (17)) have to be replaced by $A_{rel,e}$ (Eq. (10)) and $B_{rel,e}$ (Eq. (11)), respectively.

With this approach, the contraction dynamics for the eccentric branch of the force-velocity relation can be calculated in the same way as the concentric branch. Only two new parameters are required, the asymptotic force F_e and the ratio of the slopes S_e.

2.6. Required steps in a numerical simulation

The muscle tendon complex model is basically a function $F_{MTC} = F_{MTC}(l_{MTC}, \dot{l}_{MTC}, q, l_{CE}, \dot{l}_{CE})$ requiring the integration of the internal degree of freedom l_{CE} (Eq. (15)). For a numerical implementation, the following steps are required.

1. Define the initial conditions (index "i"): $l_{MTC,i}$, $\dot{l}_{MTC,i}$, q_i, and $l_{CE,i}$. We propose to begin simulations with $\dot{l}_{MTC,i} = 0$. Then, by giving $l_{MTC,i}$ and q_i, the initial state of the MTC is defined. Finally, $l_{CE,i}$ can then be derived by solving the equation $0 = qF_{isom}F_{max} + F_{PEE} - F_{SEE}$. This can be achieved in symbolic or numeric form with the constraint $0 < l_{CE,i} < l_{MTC,i}$.
2. Calculate the required model formulae in the following order to get F_{MTC}: F_{isom}, F_{PEE}, F_{SEE}, A_{rel}, B_{rel}, D_0, C_2, C_1, C_0, $\dot{l}_{CE}$. If this results in the concentric case $\dot{l}_{CE} > 0$, calculate $A_{rel,e}$, $B_{rel,e}$, $D_{0,e}$, $C_{2,e}$, $C_{1,e}$, $C_{0,e}$, and recalculate the eccentric $\dot{l}_{CE}$.
3. Calculate F_{SDE}, and finally $F_{MTC} = F_{SEE}(l_{CE}, l_{MTC}) + F_{SDE}(l_{CE}, \dot{l}_{CE}, \dot{l}_{MTC}, q)$, which is the output of the muscle tendon complex model.
4. Optional: calculate F_{CE} for evaluation purposes.
5. Integrate $\dot{l}_{CE}$ to get l_{CE} along with the ...
6. multi-body simulation that calculates the generated motion from F_{MTC}, which results in new l_{MTC}, $\dot{l}_{MTC}$, and q. Now, repeat from Step 2.

3. Eccentric force in rapid arm movements

In rapid elbow flexion movements, the extensor muscles operate in eccentric mode. By simulating rapid arm movements, we demonstrate the difference caused by the model extension.

We modeled a single joint elbow driven by two model muscles representing the major flexor and extensor muscles. Arm and muscle geometry, activation dynamics and muscle parameters are based on the work of Kistemaker et al. [14]. The arm dynamics are described by the differential equation

$$I\ddot{\varphi} = r_{\text{flex}}(\varphi) F_{\text{flex}}(l_{\text{flex}}, \dot{l}_{\text{flex}}, q_{\text{flex}}) + r_{\text{ext}}(\varphi) F_{\text{ext}}(l_{\text{ext}}, \dot{l}_{\text{ext}}, q_{\text{ext}}) \quad (20)$$

where r are the lever arms [Eq. A12 in 14] and F the muscle tendon complex forces of the flexor and extensor muscle groups (see §2.6). To generate a rapid arm movement from 45 deg to 135 deg, the flexor muscle activity level was set to $q_{\text{flex}} = 0.66$, and the extensor activity level to $q_{\text{ext}} = 0.12$. The resulting arm movement and muscle forces are shown in Fig. 5. For comparison, the same movement was also simulated with the previous muscle model [18].

The difference between the two muscle models is that with the new model the desired angle $\varphi_{\text{des}} = 135\,\text{deg}$ was reached after about 0.29 s, compared to 0.5 s in the previous model. Maximum angular velocity was $\dot{\varphi}_{\max} = 868\,\text{deg/s}$ with the new model, compared to $\dot{\varphi}_{\max} = 572\,\text{deg/s}$ with the previous model. With the new muscle model, both the resulting movement and the reached maximal velocities are more realistic with respect to human arm movements [14]. The eccentric force-velocity relation, which caused unrealistically high CE forces in rapid lengthening contractions in the previous model (comparison see Fig. 3c), is responsible for the observed difference (Fig. 5).

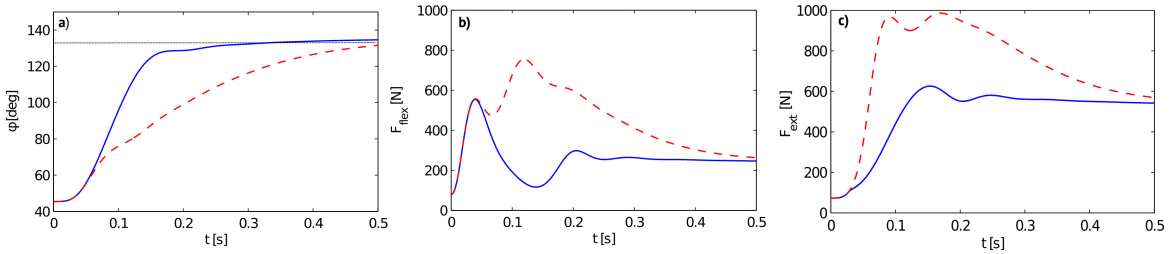

Figure 5: Results of the arm movement simulation for the new model (solid blue line) compared to the previous model (dashed red line Günther et al. [6], Mörl et al. [18]). a) The desired elbow angle $\varphi_{des} = 135\,\text{deg}$ (dashed gray) was reached faster with the new muscle model. b) Resulting muscle forces were identical during concentric contraction ($t < 0.05\,\text{s}$) in the flexor muscle, but deviated significantly during eccentric contractions, as expected from the difference shown in Fig. 3c.

4. Discussion

The extended Hill-type muscle model we presented consists of four elements: CE – a contractile element with force-length relation and force-velocity relation for concentric and eccentric contractions, PEE – parallel elastic element, SEE – series elastic element, and SDE – serial damping element. The main difference to previous models is the consideration of both serial damping [6, 18] and the eccentric force-velocity relation [27]. With this, the model is detailed enough to investigate neuro-muscular concepts (e.g. [18, 14]). At the same time, it is still reduced enough to be suitable for multi-body simulations of human and animal movement, where many muscles have to be modeled (e.g. [27]).

Although suitable for many biomechanical simulations, the model has its limitations, i.e., it does not consider all known effects relevant for muscle force generation. For example, it cannot reproduce the shift of optimum muscle length to longer lengths which has been observed in experiments at submaximal muscle activation [22, 2, 19]. As most muscles operate in a range shorter than or around the optimal length [3], our model will typically overestimate the muscle force at submaximal activation. This has to be considered if simulation of submaximal contractions is intended. Furthermore, the current model cannot reproduce contraction history effects [17, 21, 16, 26], recruitment patterns of slow- and fast twitch fibers [28], or the muscles' internal mass distribution and dynamics [7]. Such effects and properties can be considered in future model extensions. We therefore provide the muscle model as Matlab/Simulink code under the BSD-License (see electronic supplementary material) to be used in further studies.

Conflict of interest statement

None.

[1] Alexander, R. M. Damper for bad vibrations. *Nature*, 414(6866):855–7, 2001. doi: 10.1038/414855a. PMID 11780044.

[2] Brown, I. E., Cheng, E. J., and Loeb, G. E. Measured and modeled properties of mammalian skeletal muscle. II. The effects of stimulus frequency on force-length and force-velocity relationships. *Journal of Muscle Research and Cell Motility*, 20(7):627–43, 1999. doi: 10.1023/A:1005585030764. PMID 10672511.

[3] Burkholder, T. J. and Lieber, R. L. Sarcomere length operating range of vertebrate muscles during movement. *The Journal of experimental biology*, 204(Pt 9):1529–36, 2001. PMID 11296141.

[4] Cole, G. K., van den Bogert, A. J., Herzog, W., and Gerritsen, K. G. Modelling of force production in skeletal muscle undergoing stretch. *Journal of Biomechanics*, 29(8):1091–1104, 1996. doi: 10.1016/0021-9290(96)00005-X.

[5] Günther, M. and Ruder, H. Synthesis of two-dimensional human walking: a test of the lambda-model. *Biological Cybernetics*, 89(2):89–106, 2003. doi: 10.1007/s00422-003-0414-x. PMID 12905038.

[6] Günther, M., Schmitt, S., and Wank, V. High-frequency oscillations as a consequence of neglected serial damping in Hill-type muscle models. *Biological Cybernetics*, 97(1):63–79, 2007. doi: 10.1007/s00422-007-0160-6. PMID 17598125.

[7] Günther, M., Röhrle, O., Haeufle, D. F. B., and Schmitt, S. Spreading out Muscle Mass within a Hill-Type Model: A Computer Simulation Study. *Computational and Mathematical Methods in Medicine*, 2012:1–13, 2012. doi: 10.1155/2012/848630.

[8] Haeufle, D. F. B., Grimmer, S., and Seyfarth, A. The role of intrinsic muscle properties for stable hopping - stability is achieved by the force-velocity relation. *Bioinspiration & Biomimetics*, 5(1):016004, 2010. doi: 10.1088/1748-3182/5/1/016004.

[9] Hill, A. V. The heat of shortening and the dynamic constants of muscle. *Proceedings of the Royal Society of London. Series B*, 126(843):136–195, 1938. doi: 10.1098/rspb.1938.0050.

[10] Houdijk, H., Bobbert, M. F., and de Haan, A. Evaluation of a Hill based muscle model for the energy cost and efficiency of muscular contraction. *Journal of Biomechanics*, 39(3):536–43, 2006. doi: 10.1016/j.jbiomech.2004.11.033. PMID 16389094.

[11] Joyce, G. and Rack, P. Isotonic lengthening and shortening movements of cat soleus muscle. *The Journal of physiology*, 204(2):475–491, 1969.

[12] Katz, B. The relation between force and speed in muscular contraction. *The Journal of Physiology*, 96(1):45–64, 1939.

[13] Ker, R. F. Dynamic tensile properties of the plantaris tendon of sheep (Ovis aries). *The Journal of Experimental Biology*, 93(1981):283–302, 1981. PMID 7288354.

[14] Kistemaker, D. a., Van Soest, A. J., and Bobbert, M. F. Is equilibrium point control feasible for fast goal-directed single-joint movements? *Journal of Neurophysiology*, 95(5):2898–912, 2006. doi: 10.1152/jn.00983.2005. PMID 16436480.

[15] Lindstedt, S. L., LaStayo, P. C., and Reich, T. E. When active muscles lengthen: properties and consequences of eccentric contractions. *News in Physiological Sciences*, 16(3):256–61, 2001. PMID 11719600.

[16] McGowan, C. P., Neptune, R. R., and Herzog, W. A phenomenological muscle model to assess history dependent effects in human movement. *Journal of Biomechanics*, 46(1):151–7, 2013. doi: 10.1016/j.jbiomech.2012.10.034. PMID 23178037.

[17] Meijer, K., Grootenboer, H., Koopman, H., van der Linden, B., and Huijing, P. A Hill type model of rat medial gastrocnemius muscle that accounts for shortening history effects. *Journal of Biomechanics*, 31(6):555–563, 1998. doi: 10.1016/S0021-9290(98)00048-7.

[18] Mörl, F., Siebert, T., Schmitt, S., Blickhan, R., and Günther, M. Electro-Mechanical Delay in Hill-Type Muscle Models. *Journal of Mechanics in Medicine and Biology*, 12(05):1250085, 2012. doi: 10.1142/S0219519412500856.

[19] Rack, P. and Westbury, D. The effects of length and stimulus rate on tension in the isometric cat soleus muscle. *The Journal of Physiology*, 204(2):443–460, 1969.

[20] Rijkelijkhuizen, J. M., de Ruiter, C. J., Huijing, P. A., and de Haan, A. Force/velocity curves of fast oxidative and fast glycolytic parts of rat medial gastrocnemius muscle vary for concentric but not eccentric activity. *Pflügers Archiv: European journal of physiology*, 446(4):497–503, 2003. doi: 10.1007/s00424-003-1052-9. PMID 12719979.

[21] Rode, C., Siebert, T., and Blickhan, R. Titin-induced force enhancement and force depression: a 'sticky-spring' mechanism in muscle contractions? *Journal of Theoretical Biology*, 259(2):350–60, 2009. doi: 10.1016/j.jtbi.2009.03.015. PMID 19306884.

[22] Sandercock, T. G. and Heckman, C. J. Whole muscle length-tension properties vary with recruitment and rate modulation in areflexive cat soleus. *Journal of Neurophysiology*, 85(3):1033–8, 2001. PMID 11247973.

[23] Seyfarth, a., Blickhan, R., and Van Leeuwen, J. L. Optimum take-off techniques and muscle design for long jump. *The Journal of Experimental Biology*, 203(Pt 4):741–50, 2000. PMID 10648215.

[24] Siebert, T., Wagner, H., and Blickhan, R. Not all oscillations are rubbish: forward simulation of quick-release experiments. *Journal of Mechanics in Medicine and Biology*, 3(1):107–122, 2003. doi: 10.1142/S0219519403000648.

[25] Siebert, T., Rode, C., Herzog, W., Till, O., and Blickhan, R. Nonlinearities make a difference: comparison of two common Hill-type models with real muscle. *Biological Cybernetics*, 98(2):133–43, 2008. doi: 10.1007/s00422-007-0197-6. PMID 18049823.

[26] Till, O., Siebert, T., Rode, C., and Blickhan, R. Characterization of isovelocity extension of activated muscle: a Hill-type model for eccentric contractions and a method for parameter determination. *Journal of Theoretical Biology*, 255(2):176–87, 2008. doi: 10.1016/j.jtbi.2008.08.009. PMID 18771670.

[27] van Soest, A. J. and Bobbert, M. F. The contribution of muscle properties in the control of explosive movements. *Biological Cybernetics*, 69(3):195–204, 1993. doi: 10.1007/BF00198959. PMID 8373890.

[28] Wakeling, J. M., Lee, S. S. M., Arnold, A. S., de Boef Miara, M., and Biewener, A. a. A Muscle's Force Depends on the Recruitment Patterns of Its Fibers. *Annals of Biomedical Engineering*, 40(8):1708–20, 2012. doi: 10.1007/s10439-012-0531-6. PMID 22350666.

[29] Winters, J. M. *Hill-based muscle models: a systems engineering perspective*, pages 69–93. Springer-Verlag Berlin and Heidelberg GmbH & Co. K, 1990.

[30] Zajac, F. E. Muscle and tendon: properties, models, scaling, and application to biomechanics and motor control. *Critical Reviews in Biomedical Engineering*, 17(4):359–411, 1989. PMID 2676342.